

# PROCEEDINGS OF SPIE

[SPIDigitalLibrary.org/conference-proceedings-of-spie](https://spiedigitallibrary.org/conference-proceedings-of-spie)

## Imaging of the human tooth cementum ultrastructure of archeological teeth, using hard x-ray microtomography to determine age-

Gabriela Mani-Caplazi  
Georg Schulz  
Hans Deyhle  
Gerhard Hotz  
Werner Vach  
Ursula Wittwer-Backofen  
Bert Müller

# Imaging of the human tooth cementum ultrastructure of archeological teeth, using hard X-ray microtomography to determine age-at-death and stress periods

Gabriela Mani-Caplazi\*<sup>a</sup>, Georg Schulz<sup>b</sup>, Hans Deyhle<sup>c</sup>, Gerhard Hotz<sup>a,d</sup>, Werner Vach<sup>e</sup>, Ursula Wittwer-Backofen<sup>f</sup>, Bert Müller<sup>b</sup>

<sup>a</sup>Integrative Prehistory and Archaeological Science, University of Basel, Switzerland; <sup>b</sup>Biomaterials Science Center, Department of Biomedical Engineering, University of Basel, Switzerland; <sup>c</sup>X-ray Nanoimaging Group, School of Physics & Astronomy, University of Southampton, United Kingdom; <sup>d</sup>Natural History Museum of Basel, Anthropological Collection, Switzerland; <sup>e</sup>Department of Orthopaedics and Trauma Surgery, University Hospital Basel, Switzerland; <sup>f</sup>Biological Anthropology, University of Freiburg, Germany

## ABSTRACT

Tooth cementum annulation (TCA) is used by anthropologists to decipher age-at-death and stress periods based on yearly deposited incremental lines (ILs). The destructive aspect of the TCA method, which requires cutting the tooth root in sections to display the ILs, using transmission light microscopy, can be problematic for archeological teeth, and so a non-invasive imaging technique is preferred. The purpose of this study is to evaluate conventional micro computed tomography ( $\mu$ CT) and synchrotron radiation-based X-ray micro computed tomography (SR $\mu$ CT) as a non-destructive technique to explore the tooth cementum ultrastructure and to display ILs. Seven archeological teeth from the Basel-Spitalfriedhof collection (patients died between 1845 and 1868 in the city hospital) were selected for the  $\mu$ CT experiments. This collection is considered a unique worldwide reference series in the anthropological science community, due to the high level of documented life history data in the medical files and the additionally collected and verified birth history by genealogists. The results demonstrate that the conventional  $\mu$ CT is complementary to the SR $\mu$ CT allowing to prescreen the teeth using conventional  $\mu$ CT to identify the appropriate specimens and areas for the SR $\mu$ CT measurements. SR $\mu$ CT displayed cementum ring structure corresponding to the ILs in the microscope view in archeological teeth in a non-invasive fashion with the potential for more accurate assessments of ILs compared to conventional techniques. The ILs were mainly clearly visible, and it was possible to count them for age-at-death assessment and identify qualitatively irregular ILs which could constitute stress markers.

**Keywords:** Synchrotron radiation-based micro computed tomography, conventional micro computed tomography, archeological teeth, tooth cementum annulation (TCA), incremental line, dental cementum, stress marker identification, pregnancy, mineralization

## 1. INTRODUCTION

Tooth cementum annulation (TCA) is an established method for determining age-at-death by counting yearly deposited incremental lines (ILs) [1-3]. Light microscopy is the standard method for IL analysis. For this purpose, 70 to 80  $\mu$ m sections of the tooth root have to be prepared, but this destructive aspect of the TCA can be problematic for archeological teeth, and so a non-invasive imaging technique is preferred. Conventional micro computed tomography ( $\mu$ CT) and synchrotron radiation-based micro computed tomography (SR $\mu$ CT) techniques have the potential for less or non-destructive, high-resolution imaging of the tooth cementum. SR $\mu$ CT has shown promising results in displaying the ILs of a beluga whale [4] and has demonstrated to be an alternative to traditional approaches to image growth lines in dentin and enamel in fossil human teeth [5]. Cementum is a mineralized tissue covering the tooth root and is deposited lifelong supporting the anchoring of the tooth in the alveolar bone [6].

\*[g.mani@unibas.ch](mailto:g.mani@unibas.ch); phone +41 61 207 42 00; fax +41 61 207 42 55; [www.ipna.unibas.ch](http://www.ipna.unibas.ch)

Cementum has a relatively homogenous pattern, with ILs representing its phased deposition [6]. These alternating phases of cementum growth in a circannual rhythm are the result of endogenous cycles reflecting environment factors related to seasons [7, 8].

In transmission light microscopy images, an IL consists of a bright and a dark ring representing one year (Figure 1 (c)). The brighter and usually wider ring is described to correspond to periods of growth, such as summer months, while the darker and usually thinner ring is deposited during periods of rest or slower growth, such as winter months [9]. Cementum consists mainly of collagen and hydroxyapatite crystals, their concentrations and/or orientations are assumed to be responsible for the optical properties of the two types of lines [9,10]. Cementum structure and mineralization have been examined by several methods, such as scanning electron microscopy [9], transmission light microscopy [9], interference contrast microscopy [11], spectroscopy [12] and microradiography [9]. However, there is no common agreement about the cause responsible for the layered structure, though recent analyses using synchrotron X-ray fluorescence and diffraction scanning support that the dark and light bands are due to mineral density differences [13].

Irregular ILs in terms of IL width and color are regarded as stress markers (SMs) (see Figure 2) and may point to events such as a pregnancy, lactation period or disease, conditions that affect calcium metabolism [2,14]. Such SMs can be linked to a year of life by applying the TCA method. For optimal SM identification, an understanding of the tooth cementum structure is essential. The purpose of this study is to evaluate conventional and synchrotron radiation-based X-ray micro computed tomography as a non-destructive technique to explore the tooth cementum ultrastructure, in order to display the ILs and to contribute to the understanding of irregular ILs and the three-dimensional identification of SMs. This study is part of a more comprehensive investigation seeking to identify irregular ILs (SMs), using an adapted TCA method, and assessing the correlation between these SMs and known life history events. The teeth analyzed in this study are from the Basel-Spitalfriedhof collection from the nineteenth century, which is a unique worldwide reference series in the anthropological science community, due to the high level of documented life history data in medical files and additionally collected and verified birth history by genealogists [15].

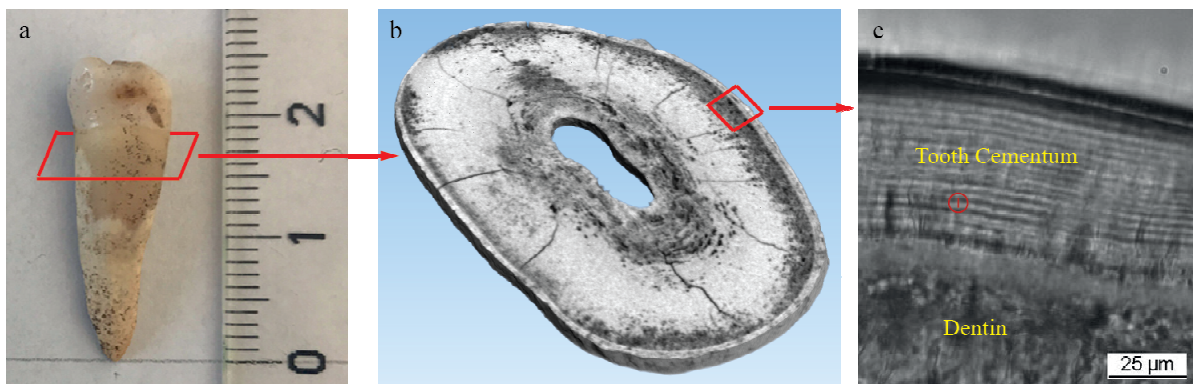


Figure 1. (a) Mandibular premolar with the cross-section in the tooth root indicated. (b) Conventional three-dimensionally (3D)  $\mu$ CT scan with a pixel size of  $5 \mu\text{m}$  showing the virtual cross-section of the tooth root, with tooth cementum in the outermost part of the root. (c) Microscopic view ( $\times 400$  magnification) of the tooth cementum of a mandibular canine; the vector presents an IL.

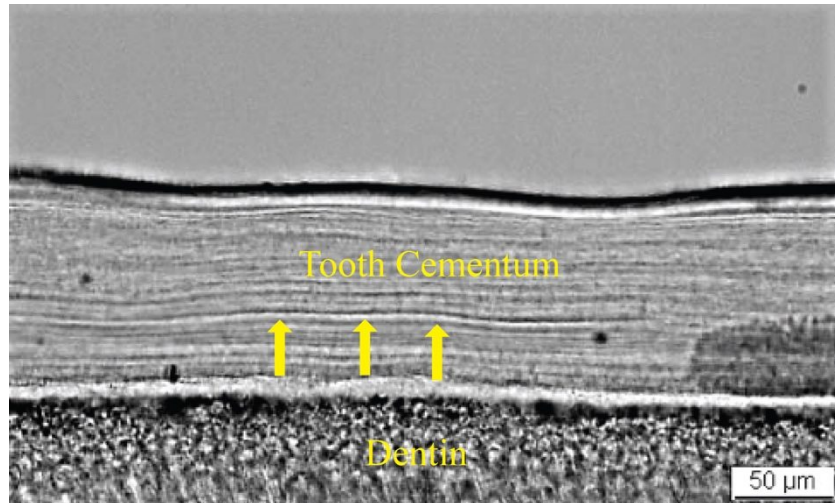


Figure 2. Microscopic view ( $\times 200$  magnification) of the tooth cementum of a mandibular canine (Z-436) from Maria Eva Kalchschmidt (November 26, 1802 – August 20, 1851). Arrows indicate an irregular IL.

## 2. METHODS

### 2.1 Specimen selection and preparation

Seven permanent human teeth (canines or premolars) were analyzed using high-resolution micro computed tomography experiments (six teeth from women with documented births and one tooth from a man). The archeological teeth are from the highly documented Basel Spitalfriedhof collection in Switzerland (stored at the Natural History Museum Basel), from the nineteenth century as described in the introduction. The patients lived during the early industrialization and one or more transcribed medical records (stored in the township archives at Staatsarchiv Basel-Stadt) were available for each identified skeleton, depending on the number of hospital stays. The dates of birth and age-at-death of the selected patients were verified [15, 16]. The patients were buried between 1845 and 1868 and excavated in 1988 and 1989 by the archeological Bodenforschung Basel-Stadt. Geographical and social origins and family situations for three generations (parents, the selected individual and the next generation) were confirmed genealogically and historically [17, 18]. The number of births and birth intervals were evaluated and validated according to different church archives (baptism, marriage, confirmation and funeral). This high-level patient information, including birth history, allows to compare the identified SMs with the documented life history data.

The tooth cementum, which is optimal for TCA, is the acellular extrinsic fiber cementum (AEFC) that extends from the cervical margin of the tooth root, covering around two-thirds [19] of the root. Its diameter ranges from 30 to 230  $\mu\text{m}$  [20]. The cervical part of the middle-third area of the tooth root (Figure 1 (a)) has to be scanned in line with the area to be sectioned for TCA [1], using conventional  $\mu\text{CT}$  and SR $\mu\text{CT}$ .

### 2.2 Micro computed tomography

#### 2.2.1 Conventional micro computed tomography

Altogether, six teeth (three teeth prescreened for SR $\mu\text{CT}$  and three teeth sectioned for higher resolution measurements) were scanned using the conventional lab-based  $\mu\text{CT}$  scanner nanotom® (GE Sensing & Inspection Technologies GmbH, Wunstorf, Germany) to display the cementum layer and to find interesting regions for SR $\mu\text{CT}$  measurements. The scans were performed with a pixel size of 5 to 10  $\mu\text{m}$ , and 1200 equiangular radiographs were recorded over 360° with a 3-second exposure time per projection. For the experiments, an acceleration voltage of 90 kV and a beam current of 200  $\mu\text{A}$  were selected.

#### 2.2.2 Synchrotron radiation-based micro computed tomography

Four intact teeth (two of the three teeth prescreened by the lab-based  $\mu\text{CT}$  and two teeth that had not been prescreened) were scanned at the beamline ID 19 (ESRF, Grenoble, France). One tooth (Z-1584, a maxillary premolar of a 36-year-old woman, with one documented birth) was selected for a comprehensive synchrotron analysis. Measurements were

performed in local tomography geometry with mean photon energy of 19.5 keV (pink beam). Exposure time was 0.1 second per projection. The propagation distance between the specimen and the detector was set to 10 mm, to allow for single-distance phase retrieval (Paganin [21]) before reconstruction. Due to the periodicity of the incremental lines of 2 to 3  $\mu\text{m}$ , an effective detector pixel size below 0.5  $\mu\text{m}$  was selected. Overview scans with 0.66  $\mu\text{m}$  pixel size were performed to identify a suitable region for further investigation. The selected regions were then scanned at a pixel size of 0.33  $\mu\text{m}$ , following which 3001 projections over  $360^\circ$  were acquired. Only a small part of the cementum could be displayed by one scan. Therefore, several scans were required to cover a relevant part of the cementum. Five local tomography positions in the virtual transverse sections were scanned to find an appropriate area where ILs could be identified (Figure 3 (b)). Applying three height steps per local position, with a pixel size of 0.33  $\mu\text{m}$  and  $2000 \times 2000$  pixels per projection, allowed to scan a root height of 2 mm. Fifteen scans were acquired altogether from the preselected tooth.

### 3. RESULTS

#### 3.1 Conventional micro computed tomography

Below we present pictures of one tooth that was measured comprehensively and selected for SR $\mu$ CT. Figure 3 (a) shows a 3D rendering of the complete tooth from the conventional  $\mu$ CT scan, while Figure 3 (b) illustrates a reconstructed slice of this tooth with a pixel length of 5  $\mu\text{m}$ . The tooth cementum is located in the outer part, distinguished from the subjacent dentin. The cementum has a width ranging from 80 to 110  $\mu\text{m}$  and appears brighter compared to the dentin, meaning that it has a higher X-ray absorption compared with the less dense dentin. This tooth shows alterations in dentin and cementum over a wide area of the tooth root, which could constitute a challenge to display ILs when using SR $\mu$ CT. However, due to the clearly visible cementum showing a relatively uniform width over the cross-section, this tooth was selected for the comprehensive SR $\mu$ CT measurements. The other two teeth screened by conventional  $\mu$ CT showed a rather thin cementum width, considering the patients' age-at-death. Moreover, in one of those teeth, discontinued cementum was visible, so these teeth were not measured comprehensively by SR $\mu$ CT.

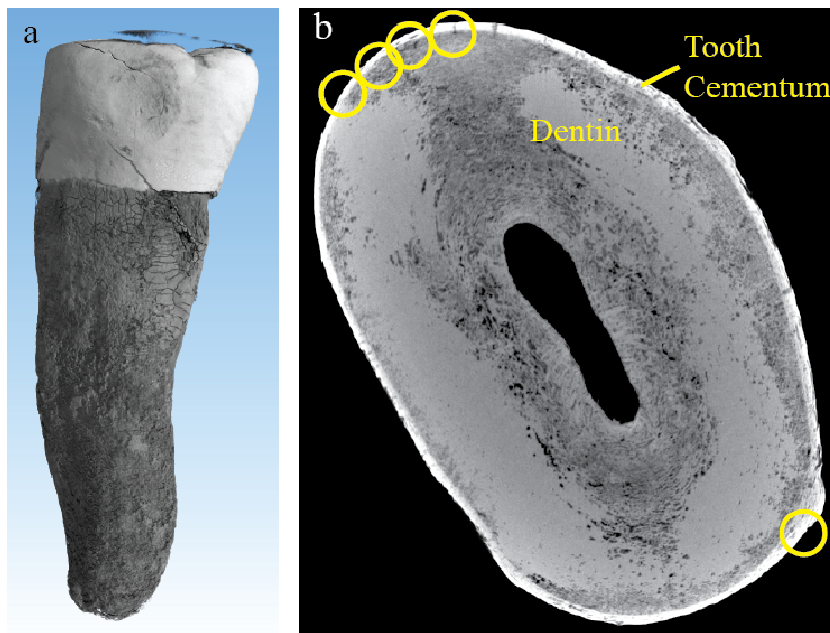


Figure 3. (a) 3D rendering of the complete tooth from the conventional  $\mu$ CT scan and (b) a selected reconstructed slice from the conventional  $\mu$ CT. The yellow-colored circles indicate the positions of the high-resolution tomography performed at the synchrotron radiation facility.

### 3.2 Synchrotron radiation-based micro computed tomography

All of the teeth measured using SR $\mu$ CT were intact. Figure 4 shows a slice through the data measured at the beamline ID19 with a pixel length of 0.66  $\mu\text{m}$ . Prior to tomographic reconstruction, single-distance phase retrieval was performed on the projections [21]. In this overview scan, cementum in the outer part can be distinguished from the dentin. In the dentin and cementum, alterations that were already visible in the conventional  $\mu$ CT view appear as round structures and are less dense than the surrounding tissue. These alterations are visible vertically in all scans. The ring structure is not yet clearly visible in this resolution.

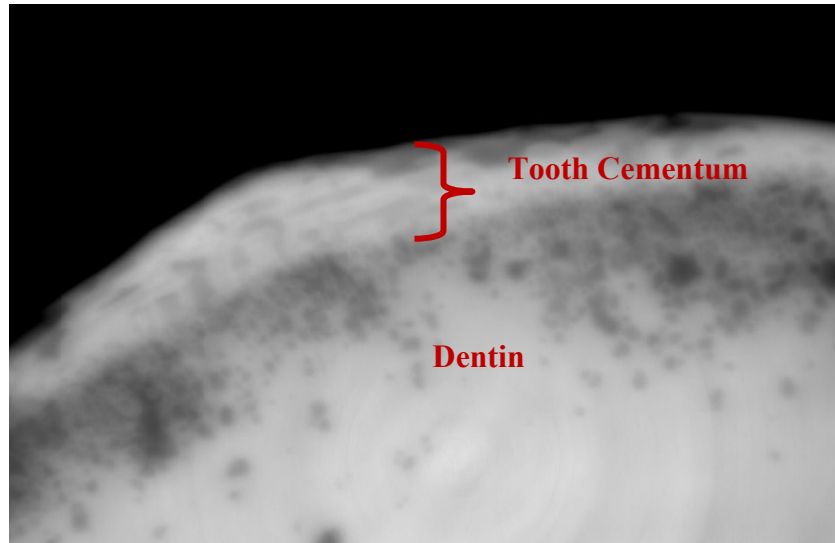


Figure 4. A propagation-based phase contrast SR $\mu$ CT overview scan showing the tooth cementum with a pixel length of 0.66  $\mu\text{m}$ , with cementum in the outer part indicated by the curly bracket distinguished from the subjacent dentin.

Figure 5 shows the same tooth with a pixel length of 0.33  $\mu\text{m}$ . The cementum displays a ring structure with a periodicity of around 3 to 4  $\mu\text{m}$ . The ILs were mainly clearly distinguished, and counting them was possible in several datasets. An average of 18 ILs can be recognized in three selected scans, while one of the ILs (blue balk) appears broader compared to the other ILs. In a further tooth, not prescreened by conventional  $\mu$ CT, the ring structures could also be displayed. Generally, it was challenging to recognize precisely the start of the cementum and the first IL.

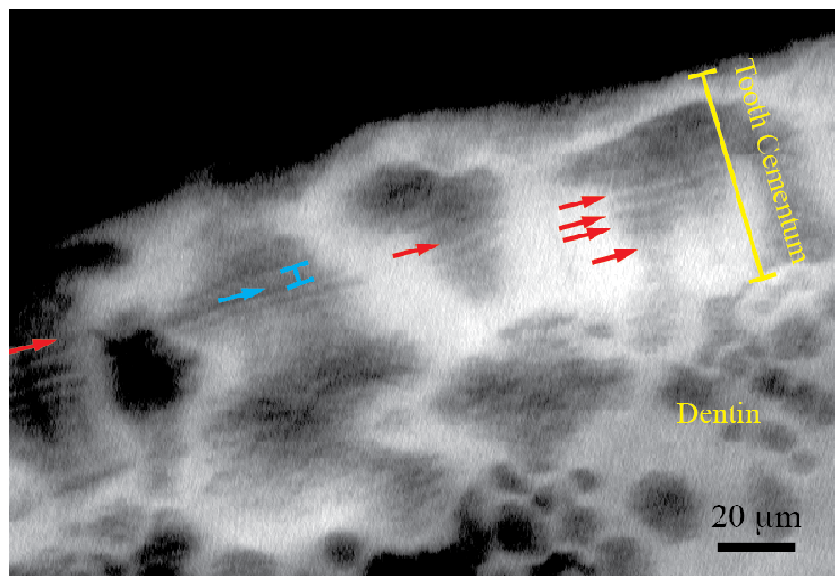


Figure 5. SR $\mu$ CT scan with a pixel size of 0.33  $\mu\text{m}$  of a premolar of a 36-year-old woman. Cementum with the ILs (red arrows) is presented, and one IL (blue arrow and balk) appears broader compared to the other ILs.

#### 4. DISCUSSION AND CONCLUSION

The SR $\mu$ CT measurements allowed to display the cementum microstructure in varying degrees of quality, along with rings that very likely correspond to the ILs in the transmission light microscope view. In the preselected tooth using conventional  $\mu$ CT, favorable areas for SR $\mu$ CT measurements were found, where the ILs were visible in the SR $\mu$ CT view over a wide part of the cementum; furthermore, it was possible to count and assess qualitatively the ILs in terms of IL width and appearance. In the deselected tooth using conventional  $\mu$ CT, no ILs were visible in the SR $\mu$ CT view. This is only a preliminary study, and further research is needed to display the ILs for accurate assessment and to understand why in some teeth it is impossible to display them. However, this issue is also known from TCA, that in some teeth or areas of the cementum, ILs are invisible.

As the magnification of conventional  $\mu$ CT is related to the positions of the source (cone-beam geometry), sample and detector, the highest resolutions can be adjusted by positioning the sample close to the source. Therefore, tooth sticks of a few millimeters in size had to be sectioned, to be able to scan at pixel sizes below 1  $\mu$ m. However, even in the sectioned teeth at a resolution of 0.7  $\mu$ m, the ILs could not be displayed. Due to the sizes of the sticks, energy had to be decreased, with the result that the intensity of the X-ray beam was insufficient. The consequent increase in scan time (around 9 h) resulted in blurred results, thus making the ILs invisible. The conventional  $\mu$ CT scans, however, were useful in prescreening the intact teeth by assessing the quality of the tooth cementum, such as the consistency of the full cementum width and to capture alterations that may constitute a challenge to display ILs in the SR $\mu$ CT view. Hence, favorable areas for SR $\mu$ CT examination of the intact tooth can be identified using conventional  $\mu$ CT.

The visualization of the ILs using SR $\mu$ CT shows that the cementum structure consists of mineral density modulations reflected by the ring structure corresponding to the ILs in the microscopic view. The brighter rings in the SR $\mu$ CT view absorb more X-ray radiation and are therefore denser structures compared to the darker rings. This investigation is a further evidence that ILs are based on mineral density differences, which have been described in several studies [9, 13] and linked primarily with variations in the relative mineralization mainly due to changes in the rate of cementogenesis [7]. The structural knowledge on ILs is relevant in helping understand the nature of the appositional growing, interpret differences between regular and irregular ILs and recognize the mechanism leading to irregular ILs. So far, irregular ILs that point to events such as a pregnancy or certain diseases have been described to vary in terms of width and color [2].

SR $\mu$ CT displays the ILs in a 3D view and allows to find the virtual section perpendicular to the exterior of the tooth root, which avoids the issue with the sometimes optically superimposed ILs in the microscopic view [22]. This improves the distinction – and hence the counting – of the ILs and provides accurate IL width measurements. The two teeth that were analyzed more comprehensively in this study were from women with a documented birth history, with the expectation based on earlier studies to spot irregular ILs [2,23]. During pregnancy, maternal physiology adjusts to ensure the optimized growth of the fetus and there is a high rise in several hormones. Maternal calcium homeostasis has to adapt to the high calcium demand of the fetus, with the highest demand in the third trimester [24]. It is expected that the hormones and growth factors active during pregnancy may influence tooth cementum growth and mineralization. In contrast to bone, cementum is not vascularized and rarely remodeled during life [25]. Structural changes in cementum, due to pregnancies and diseases, should therefore be preserved and accessible post mortem or after tooth extraction. In this study, it was possible to present the ILs in two teeth. In the preselected tooth, it was possible to count them, and an average of 18 ILs were recorded, which provides an age-at-death estimation of around 28 years. This, however, is lower than the actual age-at-death, but it needs to be considered that in this tooth the start of cementum and the first IL, the start of the counting, were challenging to assess. Additionally, the ring structure was not clearly visible over the full course of the cementum. These factors can influence the chances of capturing every IL and may result in a less accurate age-at-death estimation. Dividing the total width of the cementum by the periodicity of the ILs could be a way to overcome the issue of invisible ILs. In our case, this approach is not expected to improve the age-at-death estimation, as the main challenge is that the start of the cementum, as described above, is challenging to define. In the same tooth, an IL with a broader width compared to the other ILs was identified. The broader IL is located in the ninth IL. Adding the average eruption age of this tooth type, the broader IL would correspond to an age of 20 years. The tooth was from a woman with

one documented birth. Further investigations are needed to assess the reliability of this finding and the correlation with a stress period.

To date, there is no method available that can assess cementum ILs in human teeth in a non-destructive way. This pilot study demonstrates that SR $\mu$ CT has the potential to display the cementum microstructure corresponding to the ILs, by virtually sectioning the tooth root, and that SR $\mu$ CT is applicable for displaying cementum ILs in archeological human teeth. A disadvantage of  $\mu$ CT is the issue of destroying DNA in ancient material, which needs to be considered before starting any research. The conventional  $\mu$ CT examinations were complementary to SR $\mu$ CT, allowing to prescreen the teeth, in order to optimize the SR $\mu$ CT examinations. Hence, SR $\mu$ CT showed promising results in assessing age-at-death and stress periods in archeological teeth, as presented in this pilot study, in a non-invasive fashion. A contribution to the understanding of the tooth cementum structure could be provided and supports the evidence that ILs are based on mineralization differences.

It is highly desirable to determine the actual absorption values of the microanatomical features of cementum. Such a determination requires full-field tomography with monochromatic radiation. For this purpose, stitching techniques could help avoid cutting the crown [26]. The power of currently available hard X-ray tomography setups, however, is restricted, and so a related study has had to be postponed.

IL ring structures are not unique in nature. Certainly, we know these rings exist in trees (see, for example, [27]), but they are also found in mineralized tissues, for example otoliths [28], where they correspond to the day-night cycles and have been applied to determine the exact dates of radioactive fall-out as the result of testing atom bombs. Therefore, we conclude that the results of the present study may also become helpful for other areas of research.

## ACKNOWLEDGMENT

We thank the European Synchrotron Radiation Facility for their beamtime access (MD-1055), the SNSF for financial support (R'Equip Project 133802), Fredy Schmidli from the University of Basel for the technical support for the tooth preparation and especially Professor Dr. Jörg Schibler from the Department of Integrative Prehistory and Archaeological Science for the research support. Additionally, we would like to thank the Citizen Science Project BBS "Bürgerforschungsprojekt Basel-Spitalfriedhof" (<https://www.ipna.unibas.ch/bbs>), who does volunteer work, all the time-consuming basic research concerning historical sources, particularly the genealogist team, namely: Marie-Louise Gamma, Diana Gysin, Odette Haas, Ludwig Huber and Marina Zulauf (coordinating genealogist). In the same way we thank Verena Fiebig-Ebnetter, in charge of the patient-database "Bürgerspital 1840-1870", the Staatsarchiv-Basel-Stadt, Esther Baur, Hermann Wichers and team and the archeological Bodenforschung Basel-Stadt, Guido Lassau, Norbert Spichtig and team.

## REFERENCES

- [1] Wittwer-Backofen, U., "Age estimation using tooth cementum annulation," *Methods Mol. Biol.* 915, 129-143 (2012).
- [2] Kagerer, P. and Grupe, G., "Age-at-death diagnosis and determination of life-history parameters by incremental lines in human dental cementum as an identification aid," *Forensic Sci. Int.* 118, 75-82 (2001).
- [3] Grosskopf, B., "Individualaltersbestimmung mit Hilfe von Zuwachsringen im Zement bodengelagerter menschlicher Zähne," *Z. f. Rechtsmed.* 103, 351-359 (1990).
- [4] Nagji, S. Colard, T. Bertrand, B. D'Incau, E. and Brand, E., "Cementochronology, to cut or not to cut?" Annual Meeting - American Association of Physical Anthropology, Columbus, Ohio (2013).
- [5] Le Cabec, A. Tang, and N. Tafforeau, P., "Assessing developmental information of fossil hominin teeth using new synchrotron microtomography-based visualization techniques of dental surfaces and interfaces," *PLoS One.* 10, e0123019 (2015).
- [6] Schroeder, H. E., [Orale Strukturbiologie], Georg Thieme Verlag, Stuttgart, 144-166 (2000).
- [7] Lieberman, D. E., "The biological basis for seasonal increments in dental cementum and their application to archaeological research," *J. Archaeol. Sci.* 21, 525-539 (1994).



- [8] Grue, H. and Jensen, B., 1979 "Review of the formation of incremental lines in tooth cementum of terrestrial mammals," *Dan. Rev. Game Biol.* 11, 1-48. (1979).
- [9] Lieberman, D. E., "Life history variables preserved in dental cementum microstructure," *Science* 261, 1162-1164 (1993).
- [10] Cool, S. M. Forwood, M. R. Campbell, P. and Bennett, M. B., "Comparisons Between Bone and Cementum Compositions and the Possible Basis for Their Layered Appearances," *Bone*. 30, 386-392 (2002).
- [11] Caplazi, G., "Eine Untersuchung über die Auswirkungen von Tuberkulose auf Anlagerungsfrequenz und Beschaffenheit der Zementringe des menschlichen Zahnes," *Bull. Soc. Suisse d'Anthrop.* 10, 35-83 (2004).
- [12] Jermolli, S., "Elementprofil inkrementeller Zahnzuwachsringe Korrelation von Stoffwechselfvorgängen durch Analyse des Zahnzements und der Knochenkompakta," Bachelorarbeit. Fachhochschule Nordwestschweiz (2013).
- [13] Stock, S. R. Finney, L. A. Telsler, A. Maxey, E. Vogt, S. Okasinski, J. S., "Cementum structure in Beluga whale teeth," *Acta Biomater.* 48, 289-299 (2017).
- [14] Medill, S. Derocher, A. E. Stirling, I. Lunn, N. and Moses, R. A., "Estimating cementum width in polar bears: identifying sources of variation and error," *J. Mammal.* 90, 1256-1264 (2009).
- [15] Hotz, G. Zulauf-Semmler, M. Fiebig-Ebnetter, V. Schumacher, B. Meyer, L. Gysin, D. Gamma, M-L. Haas, O. Blatter, S. Blatter, R. and Gianola, A., "Neue Quellen zur Skelettserie Basel-Spitalfriedhof – Grundlagen interdisziplinärer Zusammenarbeit: Das Bürgerforschungsprojekt Basel-Spitalfriedhof," *Bull. Soc. Suisse d'Anthrop.* 21, 9-13 (2015).
- [16] Karakostis, F. A. Hotz, G. Wahl, J. Scherf, H. and Harvati, K., "Occupational manual activity is reflected on the patterns among hand entheses," *Am. J. Phys. Anthropol.* 164, 30-40 (2017).
- [17] Hotz, G. and Steinke, H., "Knochen, Skelette, Krankengeschichten. Spitalfriedhof und Spitalarchiv - zwei sich ergänzende Quellen," *B.Z.G.A.* 112, 105-138 (2012).
- [18] Pavel, M. and Kumpf, M., "Krank und Arm? Die Krankenakten des Bürgerspitals als Spiegel der Zeit. Sozio-ökonomische und epidemiologische Analysen aufgrund von 19'000 Patientendaten (1843 bis 1868) des Bürgerspitals Basel," *B.Z.G.A.* 117, (in press) (2017).
- [19] Nanci, A., [Ten Cate's Oral Histology Development, Structure & Function], Mosby Elsevier, St. Louis, 252-253 (2008).
- [20] Schumacher, G-H. Schmidt, H. Börnig, H. and Richter, W., [Anatomie und Biochemie der Zähne], Gustav Fischer Verlag, Stuttgart, New York, 221-223 (1990).
- [21] Paganin, D. Mayo, S. C. Gureyev, T. E. Miller, P. R. and Wilkins, S. W., "Simultaneous phase and amplitude extraction from a single defocused image of a homogeneous object," *J. Microsc.* 206, 33-40 (2002).
- [22] Maat, G. J. Gerretsen, R. R. and Aarents, M. J., "Improving the visibility of tooth cementum annulations by adjustment of the cutting angle of microscopic sections," *Forensic Sci. Int.* 159, 95-99 (2006).
- [23] Künzie, M. und Wittwer-Backofen, U., "Stress markers in tooth cementum caused by pregnancy," Annual Meeting - American Association of Physical Anthropologists, Columbus, Ohio (2008).
- [24] Naylor, K. E. Iqbal, P. Fledelius, C. Fraser, R. B. and Eastell, R., "The effect of pregnancy on bone density and bone turnover," *J. Bone Miner. Res.* 15, 129-137 (2000).
- [25] Saygin, N. E. Giannobile, W. V. and Somerman, M. J., "Molecular and cell biology of cementum," *Periodontol.* 24, 73-98 (2000).
- [26] Müller, B. Deyhle, H. Lang, S. Schulz, G. Bormann, T. Fierz, F. and Hieber, S., "Three-dimensional registration of tomography data for quantification in biomaterials science," *Int. J. Mater. Res.* 103, 242-249 (2012).
- [27] Lautner, S. Lenz, C. Hammel, J. Moosmann, J. Kühn, M. Caselle, M. Vogelgesang, M. Kopmann, A. and Beckmann, F., "Using SR $\mu$ CT to define water transport capacity in *Picea abies*," *Proc. SPIE.* 10391, 1039118 (2017).
- [28] Müller, B. Bernhardt, R. Weitkamp, T. Beckmann, F. Bräuer, R. Schurig, U. Schrott-Fischer, A. Glueckert, R. Ney, M. Beleites, T. Jolly, C. and Scharnweber, D., "Morphology of bony tissues and implants uncovered by high-resolution tomographic imaging," *Int. J. Mater. Res.* 98, 613-621 (2007).